



## Alignment of separated patches: multiple location tags

Hiromi Akutsu<sup>a</sup>, Paul V. McGraw<sup>b</sup>, Dennis M. Levi<sup>a,\*</sup>

<sup>a</sup> *University of Houston, College of Optometry, Houston, TX 77204-6052, USA*

<sup>b</sup> *University of Bradford, Department of Optometry, Bradford BD7 1DP, UK*

Received 28 February 1997; received in revised form 13 February 1998

---

### Abstract

Gaussian and Gabor patches can be accurately localized; however, it is not yet clear which cues (or location tags) the visual system utilizes for localization. To determine the cues used in spatial alignment, we measured and modelled the perceived shifts for asymmetric Gaussian and Gabor patches over a wide range of separations, patch sizes and orientations. For Gaussian patches we observed perceived shifts that were generally consistent with that of the centroid of the envelope. For Gabor patches we found that the perceived shift depends on the carrier orientation (whether co-axial or orthoaxial with the patch arrangement), separation (in units of carrier wavelength) and patch size (number of cycles per standard deviation). Gabor patches with the carrier orthoaxial (horizontal) to the three vertically arranged patches, were similar to Gaussian patches. However, Gabor patches with the carrier coaxial (vertical) to the three vertically arranged patches resulted in perceived shifts that were consistent with a number of alternate localization primitives. The selection of primitives was dependent on mainly the separation and patch size. Our results support the suggestion that the visual system can use multiple tags for location (Hess et al., *Vis Res* 1994;34:2439–2451; Badcock et al., *Vis Res* 1996;36:1467–1472). © 1998 Elsevier Science Ltd. All rights reserved.

*Keywords:* Spatial localization; Alignment; Grating; Asymmetry; Gaussian; Gabor

---

### 1. Introduction

Veridical perception of the relative location of objects is an indispensable asset of human vision for adaptive behavior in the environment. The precision of our ability to judge the relative spatial location of visual patterns has been well documented, however, the mechanisms and stimulus features which mediate the process are not clearly understood. The present study addresses the question of which spatial features of the stimulus are used to align 2D luminance patterns.

In spatial alignment tasks with well-separated patterns, some form of local sign model related to the contrast envelope of the patterns has been suggested (Klein & Levi, 1987; Wilson, 1991; Hess & Holliday, 1992; Waugh & Levi, 1993; Levi & Waugh, 1996). However, the particular aspect of a stimulus which characterizes the location is not yet determined, though the centroid, peak, zero-crossing, the peak of the luminance distribution and the mid-point of the visible

patch have all been implicated (Hess & Holliday, 1992; Hess, Dakin & Badcock, 1994; Badcock, Hess & Dobbins, 1996; Hess & Holliday, 1996; Whitaker, McGraw, Pacey & Barrett, 1997).

In a recent study, (Whitaker et al., 1997) used novel asymmetric Gaussian windowed stimuli to examine perceived location. The asymmetric stimuli were similar to conventional Gaussian and Gabor patches except that the standard deviations either side of the mid-line were different. The advantage of using such stimuli is that spatial characteristics such as peak, centroid or zero-crossings of the luminance distribution predict different perceived shifts in position. The results demonstrated that perceived location was well described by the centroid of the stimulus envelope for both luminance-defined and contrast-defined stimuli. In contrast, (Hess & Holliday, 1996) in a similar type of experiment, concluded that centroid theory predicted perceived location for contrast-defined stimuli but not for luminance defined stimuli. The inconsistencies in these results indicate that the story may not yet be complete. Therefore, in the present paper, we revisit the question of which primitives are used for localization.

---

\* Corresponding author. Tel.: +1 713 7431888; e-mail: dlevi@eh.edu

This paper describes the results of five experiments involving a 3-patch-alignment task, in which we varied the spatial frequency, separation, patch size and orientation of the patches. In all experiments, the Gaussian envelope in the orthoaxial dimension, i.e. the direction perpendicular to that of the three patch's alignment, was manipulated to produce asymmetric Gaussian patterns following (Whitaker et al., 1997). To anticipate, our results show that: (1) multiple cues are used for localization; (2) the spatial structure in a Gabor patch can influence the alignment judgement over a limited separation range; and (3) there were significant individual differences in the perceived shifts evident with Gabor patches.

## 2. General methods

### 2.1. Apparatus

Throughout this study, all stimuli were displayed using the same techniques and equipment. An Apple Macintosh computer (Quadra 630) was used to generate and present stimuli, control experiments and collect data. Stimuli were displayed on an Apple high resolution monochrome monitor with a mean luminance of 40 cd/m<sup>2</sup>, and a frame rate of 67 Hz. The display field remained at the mean luminance except where target and reference patterns were presented. The digital image was generated in 8 bits, and the linear relationship between the digital image and the luminance pattern on the screen was controlled using a technique described by (Pelli & Zhang, 1991). The step size ensured sufficient luminance resolution for our stimuli. Monitor calibration was carried out using a Minolta photometer (Minolta LS 110), and stimulus contrast is specified in terms of the Weber definition ( $\Delta L/L_{\text{mean}}$ ).

### 2.2. Stimuli

The stimuli were either patches of sinusoidal grating in a 2D Gaussian envelope (experiments 2 and 4), 2D Gaussian patches (experiment 3) or patches of sinusoidal grating in a vertical-rectangular and horizontal-Gaussian envelope (experiments 1 and 5). The orientation of the grating was either vertical or horizontal. The stimulus always consisted of three patches, vertically aligned, with the two reference patterns vertically flanking the center pattern. For the reference patterns, the envelope was symmetric about both the horizontal and vertical axes. For the target pattern, the envelope was symmetric about the horizontal axis, but not about the vertical axis. In experiments 1 and 5, we used a vertical grating pattern with a vertical-rectangular envelope and horizontal-Gaussian envelope (referred to as a vertical grating patch), described by the equation:

$$L(x,y) = L_m \{1 + A \sin(2\pi f(x - x_0)) \times \exp(-0.5 * [(x - x_0)/\sigma]^2) * \text{Rect}(y - y_0)\} \quad (1)$$

where  $L_m$  is the mean luminance,  $A$  is the overall amplitude of the pattern,  $f$  is the spatial frequency of the sinusoid,  $x_0$  and  $y_0$  are the mid point of the stimulus in the horizontal and vertical directions, and  $\sigma$  is the standard deviation of the Gaussian envelope in the horizontal direction.  $\text{Rect}(y - y_0)$  is a rectangular function defined as  $\text{Rect}(y - y_0) = 1$  when  $|y - y_0| \leq 0.25^\circ$ , otherwise,  $\text{Rect}(y - y_0) = 0$ . For the target pattern,  $\sigma$  was varied for  $x - x_0 > 0$  or  $x - x_0 < 0$ , to introduce asymmetry.

In experiments 2 and 4, we used a vertical grating pattern in a 2D Gaussian envelope described by the following equation:

$$L(x,y) = L_m \{1 + A \cos(2\pi f(x - x_0)) * \exp(-0.5 * [(x - x_0)/\sigma_h]^2) * \exp(-0.5 * [(y - y_0)/\sigma_v]^2)\} \quad (2)$$

where  $\sigma_h$  and  $\sigma_v$  are the standard deviations of the Gaussian envelope in the horizontal and vertical direction, respectively, and other symbols are as described for Eq. (1). For the target pattern,  $\sigma_h$  was varied for  $x - x_0 > 0$  or  $x - x_0 < 0$ , to introduce asymmetry but  $\sigma_v$  was constant. Examples of the stimuli are shown in Fig. 1.

### 2.3. Procedure

A forced-choice paradigm was used to obtain psychometric functions relating perceived position to the physical offset of the stimuli. The step size and offset values were determined by pilot experiments. On each trial, the three patches were presented for 0.5 s with abrupt onset and offset. The observer's task was to indicate whether the central target was located to the left or right of the reference patterns by pressing the appropriate key. Observers were not given feedback. Two directions of asymmetry (skewed left and skewed right) with several  $\sigma$  ratios were randomly interleaved in a block. All the displays were viewed binocularly in a dimly lit room.

### 2.4. Data analysis

Throughout this study, our key measure was the point of subjective alignment (PSA), which represents the shift in perceived alignment. Probit analysis (Finney, 1971) was applied to the psychometric function to obtain the PSA (i.e. the 0.5 probability point of the function). A bootstrap method with 1000 repetitions

was used to obtain the 95% confidence intervals (CI) which are shown as error bars in the data plots (Foster & Bischof, 1991).

### 2.5. Model predictions

We derived quantitative predictions for our asymmetric Gaussian and Gabor patches. The location tags considered were peak, centroid, and zero-crossing. We focused on these features because each has been suggested in previous studies. We refer to these as the peak model, zero-crossing model and centroid model, respectively.

For all our experiments, the peak model always predicted ‘zero shift’ since the position of this feature remains constant irrespective of any stimulus asymmetry. The following equations were used to predict the perceived shifts:

$$\text{centroid} = \frac{\int_{-\infty}^{\infty} x f(x) dx}{\int_{-\infty}^{\infty} f(x) dx} = \sqrt{\frac{\pi}{2}} (\sigma_2 - \sigma_1) \quad (3)$$

$$\text{zero-crossings} = 0.5 (\sigma_2 - \sigma_1) \quad (4)$$

where  $x$  is a point in a stimulus pattern in one dimension,  $f(x)$  is a luminance level at  $x$ ,  $\sigma_1$  and  $\sigma_2$  are the standard deviations on either side of a Gaussian function. The derivation of Eq. (3) is shown in Appendix A.

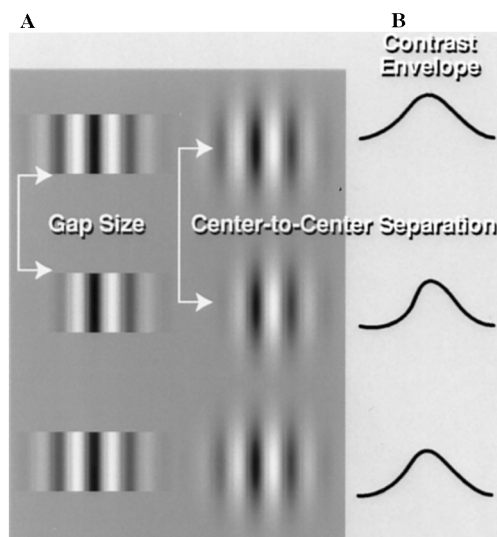


Fig. 1. (A) Examples of the three-patch stimuli. The central element is an asymmetric grating patch, and the top and bottom patches are symmetric grating patches. The left column shows three horizontal-rectangular vertical-Gaussian patches with  $\sigma$  ratio of 0.6 for the center. The right column shows three 2D Gabor patches with the same  $\sigma$  ratio for the center. In these examples, the peaks of the grating or Gabor patches are in vertical alignment, but the three patches do not appear aligned. (B) shows the contrast envelope profiles of the grating and Gabor stimuli depicted in A.

### 3. Experiment 1. Separation

When patterns are abutting or closely separated, spatial structure (i.e. carrier frequency) plays a role in relative localization, and the differential response of spatial filters is suspected as mediating alignment judgements (Klein & Levi, 1985; Wilson, 1986, 1991; Harris & Fahle, 1995). On the other hand, when the patterns are separated to some degree, it is now well established that the precision of alignment is determined mainly by the contrast envelope (Toet & Koenderink, 1988; Kooi, De Valois & Switketa, 1991; Levi & Klein, 1992; Hess & Hayes, 1994; Hess & Badcock, 1995; Levi & Tripathy, 1996). In the first experiment, we examined how the separation of the patches influences the use of cues with Gaussian patches, horizontal Gabors (with the carrier bars orthogonal to the vertically arranged patches) and vertical Gabors (with the carrier bars coaxial with the vertically arranged patches).

#### 3.1. Stimuli and procedure

The stimulus pattern was presented with a vertical-rectangular and horizontal-Gaussian envelope. The rectangular vertical envelope allowed us to vary the separation (gap) between the three patches systematically without overlap. The vertical dimension of each patch was fixed at  $0.5^\circ$  and the standard deviation ( $\sigma$ ) of the Gaussian envelope (for the symmetric Gaussian in the horizontal dimension) was fixed at  $0.5^\circ$ , containing two cycles of the carrier grating per  $\sigma$ . The grating was presented in sine phase in the envelope. For the target pattern, the ratios of the variable  $\sigma$  and the fixed  $\sigma$  were 0.8, 1.0 and 1.2. The overall position of the three patches was randomly jittered between  $-5$  and  $+5$  pixels along the horizontal axis to eliminate any frame cues. The separation of the stimulus patches, defined as the distance between the adjacent parallel borders, was varied from  $0.1$  to  $0.8^\circ$ . The contrast was fixed at 0.4, and viewing distance was 115 cm. Examples of the stimuli are shown in Fig. 1, left column.

The three stimulus patterns, no grating (i.e. a horizontal Gaussian luminance pattern), vertical grating and horizontal grating patches, were tested in separate blocks. For each condition, four offsets of the center target were presented ten times in each block. Thus, a block consisted of two directions of asymmetry, three asymmetry levels, four offsets, and ten repetitions, (240 trials), all randomly interleaved in a block. Five blocks were run. Thus, the psychometric function for one  $\sigma$  ratio was based on 400 trials. One of the authors (HA) and one naive observer (TRN) participated.

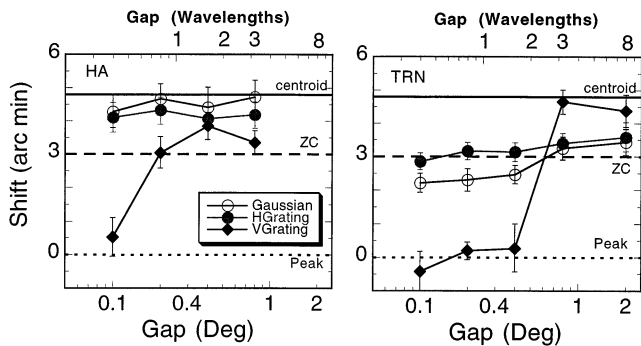


Fig. 2. Perceived shifts (in arc min) for two observers (HA and TRN) are plotted as a function of the gap size in degrees (lower abscissa) and wavelengths (upper abscissa). Each point is the average of 0.8 and 1.2  $\sigma$  ratios. The predictions of the centroid, zero-crossing and peak models are shown by horizontal lines. Symmetric patches ( $\sigma = 1.0$ ) produced no shift, thus they are omitted from the plots. Error bars represent  $\pm 95\%$  CI. While the shifts are about the same across gap sizes for Gaussian (open circles) and horizontal-grating (solid circles) patches, they varied with gap size for vertical-grating patches (diamonds).

### 3.2. Results

The results of the two observers along with the model predictions are shown as a function of the gap in Fig. 2. The perceived shift was close to either the peak (e.g. vertical gratings and small separations), zero-crossings (e.g. TRN for horizontal gratings and Gaussian patches) or the centroid (e.g. HA for horizontal gratings and Gaussian patches). The perceived shift with vertical grating patches was strongly influenced by the patch separation, while that for the Gaussian patch was much less influenced by separation. Apparently, with the coaxial (vertical) grating, there is a transition from the peak to the centroid (TRN) or zero-crossings (HA) between one and three wavelengths. This separation appears to represent the range (gap size) over which the stimulus structure can influence perceived alignment. Orthoaxial (horizontal) gratings and Gaussian patches showed very modest changes in the shift as a function of separation.

Marked differences between observers were also evident. With vertical Gabors, one observer (HA) showed a transition from zero shift to about a 3' shift (close to the zero-crossing prediction) at a separation of about one wavelength, while the other observer (TRN) showed a transition from zero shift to about a 4.8' shift (close to the centroid prediction) at a separation of about three wavelengths. When a Gaussian patch was used, HA showed shifts close to the centroid prediction, while TRN showed shifts consistent with the zero-crossing prediction.

#### 3.2.1. Statistics

A 3-way-ANOVA (two observers  $\times$  four separations  $\times$  two stimulus types) was applied to the results

with Gaussian and horizontal gratings. There was a significant difference between observers;  $F(1,3) = 661.7$ ,  $P < 0.01$ . There was no significant difference between the two patch types,  $F(1,3) = 3.93$ ,  $P > 0.1$ . Although, the main effect of separation was significant,  $F(3,3) = 14.60$ ,  $P < 0.027$ , Tukey's HSD test failed to find significant difference between any pairs. The shift averaged across all separations with Gaussian and horizontal Gabors for HA was 4.34' (95% CI 4.04–4.65'), a result which was slightly smaller than that predicted by the centroid model (4.79'). The averaged shift for TRN was 2.84' (95% CI 2.32–3.56'), consistent with the shift predicted by the zero-crossing model (3.0').

### 4. Experiment 2. Gabor patches: coarse and fine gratings

Experiment 1 showed that both the centroid of the envelope and the zero-crossings are prime candidates as stimulus primitives for well-separated patterns (Hess & Holliday, 1996; Whitaker et al., 1997); if the carrier information is not useful for the task, localization of both the Gaussian and Gabor patches may be determined by the centroid. On the other hand, if the carrier information contained in a Gabor patch is a relevant cue, the perceived shift in alignment may be smaller for a Gabor than for a Gaussian patch. For instance, one observer (TRN) might have used a bar-like feature present in the coaxial (vertical) Gabors in experiment 1. For sinusoidal grating patterns, the precision with which gratings can be localized across large gaps falls off dramatically at high spatial frequencies (Whitaker & MacVeigh, 1991). We reasoned that with windowed gratings (where both envelope and carrier cues are available) a fine grating containing many cycles might not provide useful cues for localization across a gap, whereas a coarse grating may serve this purpose. Thus, in the second experiment, we compared the effect of grating cycle number on perceived alignment of Gabor patterns. We set the separation between the patch centers at 5.5 times  $\sigma$  (i.e. either 5.5 or 11 times the wavelength). This value was chosen in part to be close to that used by Whitaker et al. (1997) who used a separation of five times  $\sigma$ .

#### 4.1. Stimuli

The stimuli were patches of sinusoidal grating windowed by a 2D Gaussian envelope, which was asymmetric in the horizontal axis. The grating was vertical and fixed in cosine phase. The separation between the centers of the patterns was fixed at 5.5 times  $\sigma$ .

The patches contained either one or two cycles of the carrier in one  $\sigma$  while  $\sigma$  was fixed at 18 pixels. These stimuli are subsequently called one- and two-cycle

Gabor patches, respectively. For the bandwidth of the stimuli, see Appendix B. Note that for the one-cycle Gabors, the center-to-center separation was equal to 5.5 times the wavelength; for the two-cycle Gabors, the center-to-center separation was equal to 11 times the wavelength. These two types of Gabor patches were viewed at either 57, 115, or 230 cm distances so that the retinal spatial frequency content varied with the retinal patch size, but the number of cycles per patch was constant. For examples of the stimulus, see Fig. 1, right column.

#### 4.2. Procedure

The  $\sigma$  ratios were 0.6, 0.8, 1.0 and 1.4 and they were varied within a single block. One- and two-cycle Gabors were tested in different blocks. One size condition was run in a block with all  $\sigma$  ratios and the polarity of asymmetry (skewed left or skewed right) interleaved in a single block. Four offset values were used to run the method of constant stimuli. For each, 50 trials were run in a block, and each block was repeated four times. Thus, each data point reported below is based on 800 trials. Two naive observers (KHN and NT) and one of the authors (HA) acted as observers.

#### 4.3. Results

There was a clear effect of grating cycle number on perceived alignment. This effect can be seen by comparing the left and right panels of Fig. 3 for each observer. Note that to facilitate comparison across different stimulus sizes, the perceived shift (in minutes) was divided by  $\sigma$  (in minutes), since it has been shown that position thresholds for similar stimuli are quite constant over a wide range of conditions when specified in  $\sigma$  units (Levi & Klein, 1990; Hess & Holliday, 1992; Levi & Klein, 1992). The two-cycle Gabor showed a stronger influence of the asymmetry than the one-cycle Gabor; the perceived shift was close to or greater than the predictions of the centroid of the stimulus for the two-cycle patch, while the results deviated from the centroid and lay closer to the predictions of the zero-crossing for one-cycle Gabor (compare the best fit lines for each). For example, for a  $\sigma$  ratio of 0.6, the shift, averaged across observers and distances was about 0.2  $\sigma$  units with a one-cycle/ $\sigma$  patch, and about 0.4  $\sigma$  units with a two-cycle/ $\sigma$  patch. Also, there were large individual differences for the one-cycle Gabor. When the shift is scaled relative to  $\sigma$ , there was no clear systematic effect of stimulus size with Gabor patches.

The slopes of the best fit lines in Fig. 3 are plotted in Fig. 4 for one- and two-cycle Gabors. The two types of stimuli differed in the number of gratings in the window as well in the separation of the patches when

defined in multiples of the spatial period of the grating (i.e. wavelength). We show the separation in terms of wavelength on the top abscissa<sup>1</sup>. Note that the center-to-center separation of 5.5–11 times the wavelength corresponds to an ‘effective gap’ of 2.5–5 times the wavelength. This is roughly the limit over which the grating cues are useful (Whitaker & MacVeigh, 1991; Whitaker, 1993). The slope of perceived shift vs.  $\sigma$  ratio was significantly higher for the two-cycle Gabor (see below). The slopes of the best fit lines and the 95% confidence intervals are presented in Table 1 along with the model predictions.

#### 4.3.1. Statistics

We applied weighted regression analysis to each observer’s data, and compared the slopes of the two stimulus types (one- and two-cycle Gabors). The slopes averaged across three observers were  $-0.41$  (95% CI  $\pm 0.11$ ) for one-cycle Gabors and  $-0.92$  ( $\pm 0.23$ ) for two-cycle Gabors. The averaged results with one-cycle Gabors are consistent with the zero-crossing model (slope of  $-0.51$ ), and those with two-cycle Gabor are consistent with the centroid model ( $-0.78$ ).

### 5. Experiment 3. Gaussian patches

Whitaker et al. (1997) found that performance was well predicted by the centroid model even for a stimulus with a large asymmetry. However, they used the same degree and polarity of skewness in a block, and this might have influenced the strategy adopted by the observers. Thus, in the third experiment, we replicated and extended the Whitaker et al.’s asymmetric Gaussian pattern experiment with naive observers by randomly varying the polarity of asymmetry of the Gaussian as well as the degree of asymmetry from trial to trial over a limited degree of asymmetry. This stimulus manipulation would make it more difficult for the observer to adopt a fixed criterion for each asymmetry, and is less prone to response bias via expectation. We also extended Whitaker et al.’s observations by varying the size of the stimulus over a 6-fold range.

Gaussian patterns do not contain spatial structure, therefore we expected the perceived shifts to be similar to those with the two-cycles Gabors, and the Gaussian patches used in the first experiment.

<sup>1</sup> When the 2D Gaussian or Gabor are used as stimulus patterns, the definition of the effective gap between the patches is not a trivial issue. Here we tentatively use 1.5 times  $\sigma$  of the Gaussian as the edge of the patches. With our 40% peak contrast stimulus, the contrast at 1.5  $\sigma$  is about 13%, and 2.0  $\sigma$  is about 5.4%, thus the visible area of the patch may be between 1.5 and 2.0  $\sigma$ . Though arbitrary, this provides a rough measure of the patch separation in terms of the grating’s spatial frequency.

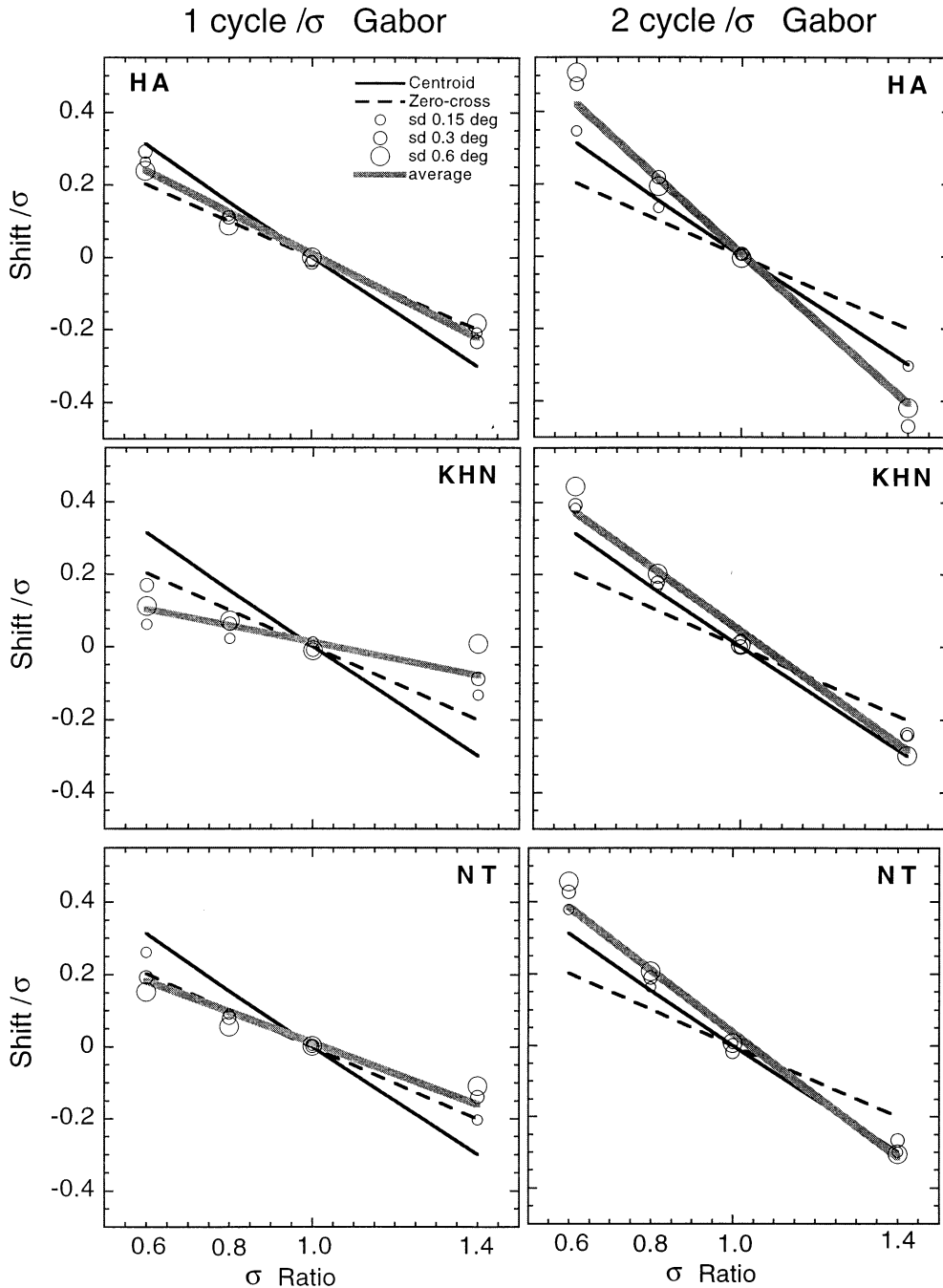


Fig. 3. Results of experiment 2. Alignment shifts for a one-cycle Gabor (left column) and two-cycle Gabor (right column) are plotted as a function of  $\sigma$  ratio, along with predictions of the centroid and zero-crossing models. Alignment shift is expressed (specified as shift/ $\sigma$ ). Different symbol sizes represent different stimulus sizes ( $\sigma = 0.15\text{--}0.6^\circ$ ). The best fit lines to the averaged data are shown by thick grey lines for each observer. The  $\pm 95\%$  CI are about the size of the largest symbol or smaller. In general, the two-cycle Gabors produced a larger shift than the one-cycle Gabors.

### 5.1. Stimuli and procedure

The stimulus patterns were identical to those used in experiment 2, except that the Gaussian windows did not contain gratings. Four Gaussian patch sizes were used, and the size was changed by varying the viewing distance, thus the separation between the patches was

constant at  $5.5 \times \sigma$ . The four Gaussian patch sizes were  $0.1^\circ \sigma$ ,  $0.15^\circ \sigma$ ,  $0.3^\circ \sigma$  and  $0.6^\circ \sigma$ . For each stimulus, 50 trials were run in a block, and each block was repeated four times. Thus, each data point reported below is based on 800 trials. Three naive observers (KHN, NT and QV), and one of the authors (HA) participated in experiment 3.

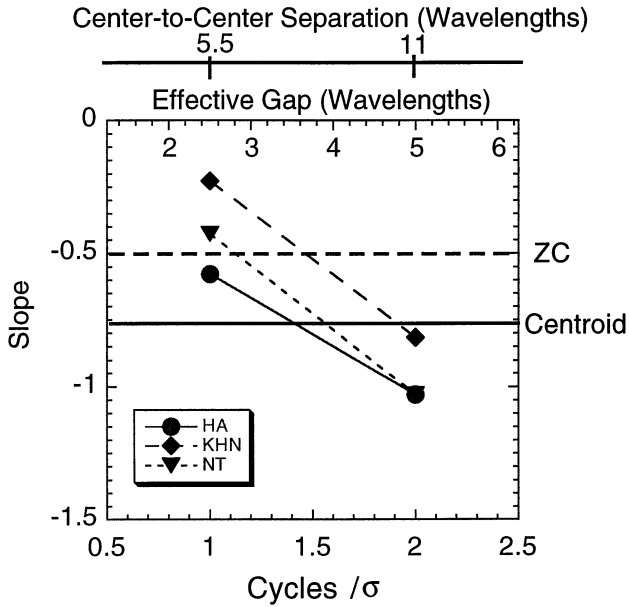


Fig. 4. The slopes of the best fit lines from Fig. 3 are plotted as a function of the number of cycles per  $\sigma$  of the Gaussian window. The slopes of the centroid and zero-crossing models are also plotted in the figure (horizontal lines). The slopes of all observers showed a similar dependence on the number of cycles. Note that the top abscissas show the center-to-center separation and the effective gap (in wavelengths).

5.2. Results

The perceived shifts are shown in Fig. 5, again, in  $\sigma$  units (specified as  $\text{shift}/\sigma$ ). Three observers (HA, KHN, and NT) showed similar results, and their perceived shifts were close to that predicted by the centroid model. The fourth naive observer (QV), consistently showed shifts between the centroid and zero-crossing predictions. There was a slight fluctuation in perceived shift among different stimulus sizes, with the smallest size typically producing slightly smaller perceived shifts.

5.2.1. Statistics

The influence of patch size was examined using regression analysis. Only subject HA revealed a significant size effect;  $F(1,13) = 8.23, P < 0.02$ . Therefore, we averaged the shift data across all sizes, and applied weighted regression analysis to estimate the slope of

shift, i.e. ( $\text{shift}/\sigma$ ), as a function of  $\sigma$  ratio. The predicted slope from the centroid and the zero-crossing models were  $-0.78$  and  $-0.51$ . The peak model predicted a slope of  $0$ . The best fit slopes and the 95% CI for each observer were as follows: HA, slope  $-0.72$ , 95% confidence interval  $(-0.58 - 0.85)$ ; KHN,  $-0.75$   $(-0.68 - 0.82)$ ; NT,  $-0.69$   $(-0.66 - 0.73)$ ; and QV,  $-0.65$   $(-0.63 - 0.67)$ . Therefore, two observers (HA and KHN) displayed shifts which were entirely consistent with the centroid model, while the other two observers (NT and QV) displayed shifts which were slightly smaller than those predicted from the centroid model. The slope averaged over the four observers was  $-0.70$  with 95% CI  $(-0.64 - 0.77)$ . This is very close to the slope of  $-0.78$  predicted by the centroid model. Thus, the results of this experiment confirm the findings of Whitaker et al. (1997) study, in that the perceived localisation of Gaussian patches can be predicted by considering the centroid of their luminance distribution.

6. Experiment 4. Gabor patches: orientation

In experiments 1 and 2, we found that the bars in the carrier of a Gabor patch can influence perceived alignment when the Gabor patch contains a small number of grating cycles. In the fourth experiment, we further tested the influence of grating structure by using two orientations: coaxial (vertical) and orthoaxial (horizontal). If the carrier plays a role in perceived alignment, the carrier orientation should also be important. For instance, the carrier should have no influence on alignment if Gabor patches with a horizontal carrier are used, since features in the horizontal direction would not be useful in judging the vertical alignment. For this stimulus, the spatial frequency in the horizontal direction is determined by the Gaussian envelope.

6.1. Stimuli and procedure

The orientation of the gratings was either vertical or horizontal. We used a fixed viewing distance (115 cm) and  $\sigma$  of the Gaussian envelope ( $0.3^\circ$  for the reference). The carrier spatial frequency was set to either 1.7, 3.3

Table 1  
Slopes of the best fit lines for average data

	One-cycle Garbor	Two-cycle Garbor	Model predictions	
			Zero-crossing	Centroid
HA	$-0.58$ ( $-0.42$ to $-0.74$ )	$-1.04$ ( $0.87$ to $-1.21$ )	$-0.51$	$-0.78$
KHN	$-0.23$ ( $-0.17$ to $-0.29$ )	$-0.82$ ( $-0.58$ to $-1.06$ )		
NT	$-0.43$ ( $-0.32$ to $-0.54$ )	$-0.89$ ( $-0.60$ to $-1.18$ )		

Average (95% confidence interval).

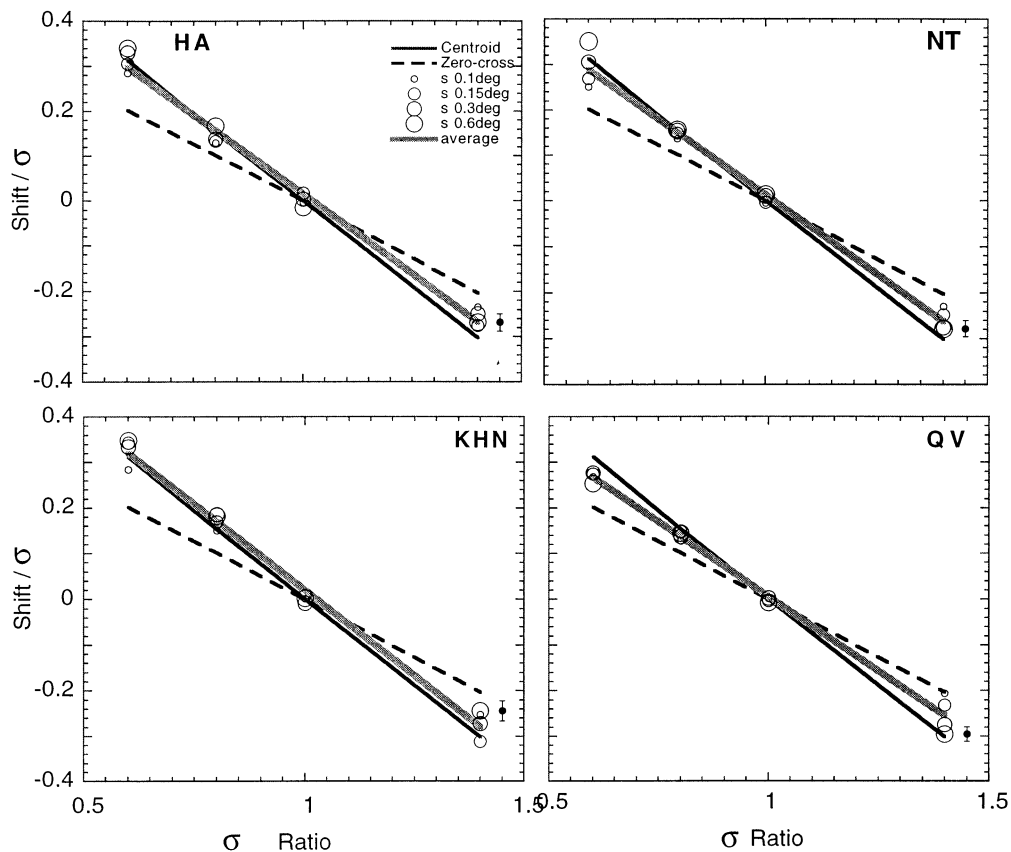


Fig. 5. Results of experiment 3. Alignment shift (specified as shift/ $\sigma$ ) is plotted as a function of  $\sigma$  ratio for each observer, along with the predictions of the two models. The best fit line for the averaged data is also shown for each observer. Different stimulus sizes ( $\sigma = 0.15$ – $0.6^\circ$ ) are shown by different symbol sizes. The averaged  $\pm 95\%$  CI is shown to the right of each plot as an error bar. The majority of the data are close to the predictions from the centroid model.

or 6.6 c/deg, and the number of cycles in one  $\sigma$  was 0.5, 1 or 2, respectively. The  $\sigma$  ratios of the asymmetric Gaussian envelopes were 0.6, 0.8, 1.0, 1.2 and 1.4. To check that the observed effect is not due to spatial frequency but due to the number of cycles, we also used a 3.3 c/deg carrier frequency with a Gaussian envelope of  $0.15^\circ$   $\sigma$  (0.5 cycle/ $\sigma$ ), achieved by doubling the viewing distance (230 cm) for the lowest spatial frequency stimulus. Two observers participated (HA and TRN). Other experimental details were as described in experiment 3.

## 6.2. Results

Fig. 6 shows the results of the two observers for vertical Gabors and horizontal Gabors, separately. The results are presented separately for Gabors with 0.5 cycle carrier in one  $\sigma$  (top panels) and one or two cycles in one  $\sigma$  (bottom panels). It is evident from the plots that when the number of cycles/ $\sigma$  was 0.5, the orientation of the carrier had a strong influence on the perceived shift; the shift was close to the predictions of the centroid model with horizontal Gabors, whereas it was close to the zero-crossing with vertical Gabors (see the

top two panels in Fig. 6). The slope of the perceived shift vs.  $\sigma$  ratio function was larger for orthoaxial (horizontal) Gabors than for coaxial (vertical) Gabors for both observers (the slopes and 95% CI of the best fit lines are shown along with the model predictions). We also found that Gabors with a 3.3 c/deg carrier and  $0.3^\circ$   $\sigma$  produced the same shift as those with a 1.65 c/deg carrier and  $0.15^\circ$   $\sigma$  for all cases in Fig. 6. When the Gabor contained one or two cycles in one  $\sigma$ , the difference between the two orientations was markedly diminished (HA) or disappeared (TRN) (see the bottom two panels in Fig. 6). Thus, the results confirm that the number of cycles/ $\sigma$  is an important factor.

### 6.2.1. Statistics

Regression analysis was applied to the perceived shifts, as no difference was found between the 95% CI across  $\sigma$  ratios in the bootstrap analysis. The data from 0.5 cycle carrier in one  $\sigma$  and one or two cycles carrier in one  $\sigma$  were analyzed separately for each observer. From Table 2, it is evident that only the vertical Gabors of 0.5 cycle /  $\sigma$  produced small shifts (i.e. flatter slopes of the regression lines), and all other stimuli produced the predictions by the centroid model or steeper.

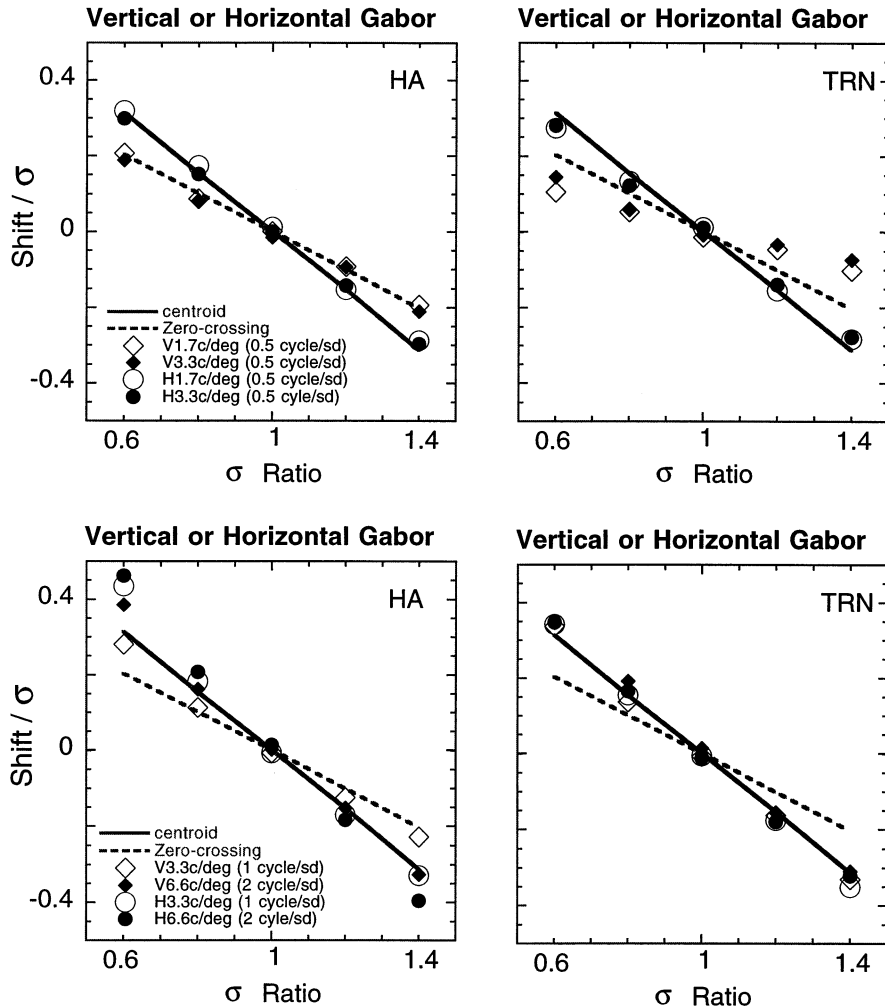


Fig. 6. Results of experiment 4. Alignment shifts (specified as shift/ $\sigma$ ) with different carrier spatial frequencies and orientations are plotted as a function of  $\sigma$  ratio for the two observers, along with the predictions of the two models. Top panels (0.5 cycle/ $\sigma$ ): For vertical Gabors, the Gabors of 1.65 c/deg with 0.15  $\sigma$  and 3.3 c/deg with 0.3  $\sigma$  produced identical perceived shifts, and they are close to (HA) or smaller than (TRN) the predictions of the zero-crossing model. For horizontal Gabors, the shifts were close to those predicted by the centroid model. Bottom panel (one and two cycles/ $\sigma$ ): When the Gabor contained one or two cycles of grating in one  $\sigma$ , the difference between the vertical Gabors and horizontal Gabors diminished or disappeared.

## 7. Experiment 5. Separation revisited

The number of cycles in the contrast envelope and the separation between envelopes both appear to be relevant factors in three-patch Vernier alignment tasks. In experiments 2 and 4, the number of cycles and the separation in terms of wavelength were confounded. With our stimulus, the number of cycles in the window was proportional to the size of the separation defined by wavelength. It is plausible that the separation, defined in terms of wavelength, is a major factor governing the use of grating information (Whitaker & MacVeigh, 1991; Whitaker, 1993). In the final experiment, we examined this possibility.

### 7.1. Stimuli and procedure

We used four envelope sizes: 0.14, 0.28, 0.42 and 0.56 deg, corresponding to 0.46, 0.92, 1.39 and 1.82 cycles of four vertical grating of 3.3 c/deg in sine phase. The  $\sigma$  ratios of the asymmetric Gaussian envelopes were 0.6, 1.0 and 1.4 for all envelope sizes. To make the gap size explicit, we again used the vertical-rectangular horizontal-Gaussian stimuli (Fig. 1 left). The gap size of the stimulus patches (defined as the distance between the adjacent parallel borders) was varied from 0.5 to 4.0 times wavelengths. Two observers participated (HA and KL); one observer (KL) was naive to the purpose of the experiment. Other experimental details were identical to those described in experiment 1.

Table 2  
Slopes of the best fit lines

	Vertical Gabor	Horizontal Gabor	Model predictions	
			Zero-crossing	Centroid
<i>0.5 cycle/σ</i>				
HA	−0.48 (−0.44 to −0.52)	−0.76 (−0.71 to −0.79)	−0.51	−0.78
TRN	−0.26 (−0.20 to −0.32)	−0.70 (−0.66 to −0.74)		
<i>1 or 2 cycles/σ</i>				
HA	−0.75 (−0.64 to −0.86)	−1.0 (−0.92 to −1.08)	−0.51	−0.78
TRN	−0.82 (−0.78 to −0.86)	−0.85 (−0.82 to −0.88)		

Average (95% confidence interval).

## 7.2. Results

Although there are large quantitative differences in perceived shift between the two observers, gap size in wavelength units, and the number of cycles in a window (represented here by  $\sigma$  size) both seem to contribute to perceived shift (see Fig. 7). Regression analysis shows that both separation and  $\sigma$  size were significant (For separation, subject HA,  $t = 2.62$  with  $df(18)$ ,  $P < 0.05$ ; for  $\sigma$  size,  $t = 9.06$  with  $df(18)$ ,  $P < 0.01$ . For separation, subject KL,  $t = 3.83$  with  $df(18)$ ,  $P < 0.02$ ; for  $\sigma$  size,  $t = -4.32$  with  $df(18)$ ,  $P < 0.02$ ). KL did not show a large overall perceived shift, the maximum shift being close to that predicted by the zero-crossing model.

When the gap size is small, grating cues may be used, especially if the pattern contains a small number of cycles. When the separation is large, the grating cues may not as useful, though differences in perceived shift due to the window size appear to persist. These results are qualitatively consistent with the results of experiment 1. We conclude that both gap (specified in wavelength units) and the number of cycles contained in the window influence the range over which grating cues can be used. Cognisance of the large individual differences dictates that formulating a functional relationship between separation, the number of cycles in the window, and perceived shift is premature.

## 8. General discussion

To summarize the results of our series of experiments, we found that: (1) Over the limited range of skewness (0.6–1.4  $\sigma$  ratio) that we tested, alignment with Gaussian patches was close to the predictions of the centroid model; (2) for orthoaxial (horizontal) Gabor patches, where the carrier is not helpful in making the vertical alignment judgement, the results were generally similar to those obtained with Gaussian patches; (3) whilst the perceived shift of Gaussian

patches and horizontal grating patches was not affected by separation, coaxial (vertical) Gabor patches with a few carrier cycles did show a marked sensitivity to separation; (4) when well-separated, coaxial (vertical) Gabor patches contain only a few carrier cycles, the observed shift was either between the predictions of the centroid and zero-crossing models or closer to the zero-crossing model; Gabor patches with several visible cycles produced perceived shifts close to or greater than the centroid model; and (5) there were substantial individual differences in the perceived shifts with vertical Gabor patches. Fig. 8 summarizes the main results of our five experiments. This figure can be viewed as a score card to illustrate the experimental conditions that favor the use of particular cues.

### 8.1. Stimulus primitives for alignment of separated patches

A large body of the results in the present experiments are accounted for by the predictions of the centroid and zero-crossing models, the main exceptions being for coaxial (vertical) Gabors containing coarse gratings.

Contrary to the suggestion of Hess and Holliday (1996), but in agreement with Whitaker et al. (1997), we find that observers use the stimulus centroid as a primitive for spatial alignment of Gaussian patterns over the range of asymmetries investigated. The range of asymmetry we used was smaller than that used by Whitaker et al. (1997). Marked individual differences, possibly related to the strategies of alignment judgement, and large asymmetries may explain the discrepancies between our results and those of Hess and Holliday (1996) and Whitaker et al. (1997). Our pilot experiments revealed that when the degree of asymmetry is large, the centroid model did not hold. It is possible that the data of Hess and Holliday (1996) did not agree with the centroid model due to the large asymmetries they used. For a limited range of asymmetry (Fig. 4C,D), their data for Gaussian patterns appear consistent with the centroid model.

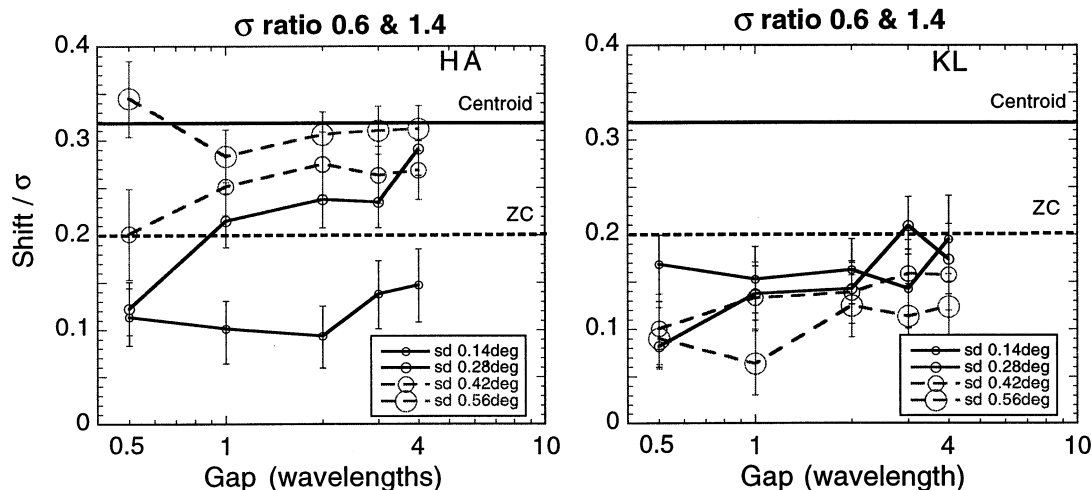


Fig. 7. Results of experiment 5. Alignment shifts (specified as shift/ $\sigma$ ) are plotted as a function of gap size for different envelope sizes (coded by symbol size) along with the predictions of two models. Each datum is based on 300 trials. For subject HA, the effects of separation and  $\sigma$  size (i.e. the number of cycles in the window) are evident.

### 8.2. Individual difference with Gabor patches

We found significant individual differences when vertical Gabor patches contained coarse gratings. For example, there were marked individual difference with one-cycle Gabors in experiment 2 (Fig. 3). HA and NT showed shifts close to the zero-crossing predictions, while KHN showed smaller shifts. A similar inconsistency was found between HA and TRN in experiment 4 (Fig. 6). This individual difference is much diminished for two-cycle Gabors or horizontal Gabors. We suspect that different observers attended to different aspects of the stimuli for coarse gratings. On the other hand, Gaussian patches produced the most consistent results of all the stimuli (see Figs. 5 and 8).

### 8.3. Are Gaussian and Gabor patches the same?

The results for Gaussian and horizontal Gabors, whose spatial structure is not useful in the vertical alignment task, were similar. However, vertical (orthogonal) Gabor patches produced qualitatively different results. For a Gabor patch, the number of cycles in the patch and the effective separation (specified in terms of wavelength), rather than the retinal spatial frequency content, plays an important role. This was clearly demonstrated in Fig. 6 (top panels); 1.65 and 3.3 c/deg Gabors produced identical shifts when the number of cycles was kept constant. With our stimulus, the number of cycles in the window was proportional to the size of the separation in terms of wavelength. Since the size of the visible area of a Gabor patch is not well defined, we cannot infer the exact separation between adjacent visible areas, however, it was roughly estimated to be between two and three wavelengths for the coarse gratings used in experiment 2 ( $5.5 \sigma - (1.5$

$\sigma * 2) = 2.5 \sigma$ , setting  $1.5 \sigma$  as the visible size). Studies by Whitaker and his colleagues suggest that the separation in terms of the grating wavelength is a critical factor in determining the use of the grating information (Whitaker & MacVeigh, 1991; Whitaker, 1993). Our results in experiment 5 rather suggest that it is more likely that both the separation defined by wavelength as well as the number of cycles in the window are factors governing the use of grating information. Hess and Holliday (1996) used Gabor patches which contained several cycles (in one  $\sigma$ ) of a 10 c/deg grating (i.e. a large separation in terms of wavelength of the carrier). Under this condition we cannot expect the carrier information to play a role in determining perceived alignment. Whitaker et al. (1997) introduced a random phase shift to the carrier in each trial, rendering grating cues useless. When the carrier information is not available, an asymmetric Gabor patch produces a large perceived shift, consistent with the centroid model (Fig. 8).

### 8.4. Is a bar or zero-bounded region used?

There may be several possible accounts for the smaller shift with coarse gratings in Gaussian envelopes. First, the peak of a bar-like structure of the patch could provide an important cue for alignment. If an observer could use the peak of a bar-like structure of the 3.3 c/deg Gabor patch, the shift should be zero, which was the case for subject TRN in experiment 1. However, another observer (HA) showed substantial shifts in the same experiment. (see also the results for HA and NT in Fig. 3). Therefore, the peak of a bar-like structure may not be the only cue used in the alignment task with coarse gratings. Secondly, the centroid computation may be performed over a limited extent of the

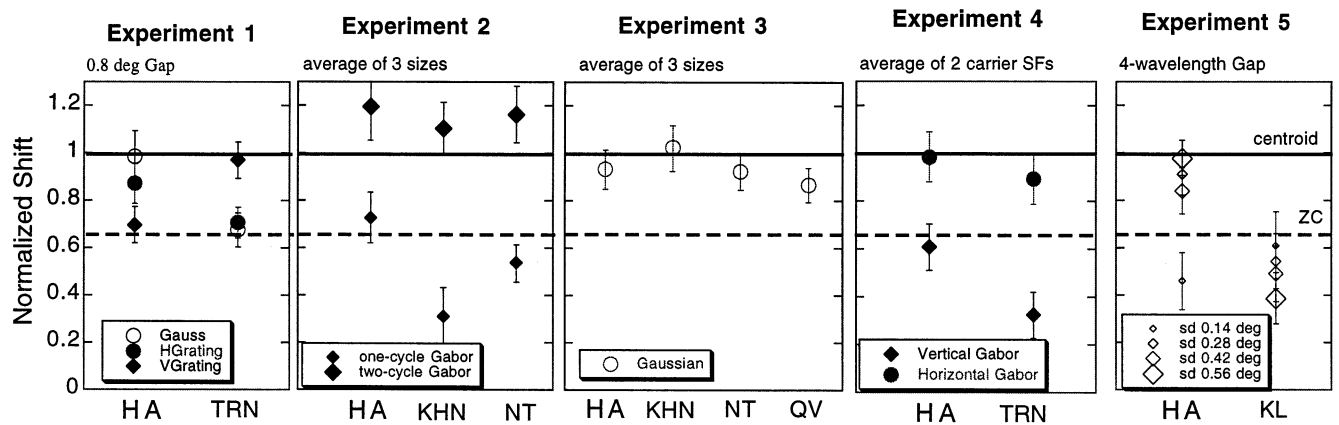


Fig. 8. Summary plots of all experiments. Averaged perceived shifts are normalized by the shift predicted by the centroid model. The solid horizontal line at 1.0 represents the shift predicted by the centroid model. The dashed horizontal line at 0.63 represents the shift predicted by the zero-crossing model. All error bars are  $\pm 95\%$  CI. Experiment 1, shifts at  $0.8^\circ$  separation are plotted for three stimulus types. Experiment 2, shifts averaged across three stimulus sizes are plotted for one- and two-cycle Gabors. Experiment 3, shifts averaged across three stimulus sizes are plotted. Experiment 4, shifts averaged across two carrier frequencies (1.65 c/deg with  $0.15 \sigma$  and 3.3 c/deg with  $0.3 \sigma$ ) are plotted for vertical and horizontal Gabors. Experiment 5: shifts at a separation of four wavelengths are plotted for four envelope sizes. Shifts with Gaussian and horizontal Gabor patches were close to the centroid in most cases, and shifts with some vertical Gabors were close to the zero-crossings. In addition, the summary plots clearly show the variance between observers.

stimulus; the wave structure may serve to ‘truncate’ the luminance pattern based on local features (such as peaks or zero-crossings in the second derivative) if the grating is low frequency or spatially sparse. This would result in a smaller shift than computed from the entire area of the stimulus.

### 8.5. Multiple tags

We found that human observers can use multiple spatial tags for stimulus localization. Considering the rich spatial structure of a Gabor patch with suprathreshold perceptual properties, namely peaks of gratings, and bar like features, the variety of cues actually used for localization is perhaps not surprising (Hess et al., 1994; Badcock et al., 1996).

## 9. Conclusion

We conducted a series of experiments using the paradigm of asymmetric patch Vernier alignment. The centroid and zero-crossing models accounted for the observers’ performance across a wide range of conditions. However, human observers seem able to use multiple spatial cues when performing relative localization tasks, the selection of cue being dependent on both the spatial characteristics of the stimulus and the observer’s strategy.

## Acknowledgements

We are grateful to David Whitaker and his collaborators for showing us their manuscript before publication and providing us with useful suggestions. This work was funded by a Research grant (RO1EY01728) to DML and a Core Center Grant P30EY07551 to UHCO from the National Eye Institute, NIH, Bethesda, MD. PVM was supported by an award from the Scottish International Education Trust and a Vision Research Training Fellowship from the Wellcome Trust, UK.

## Appendix A

Analytical solution for the centroid of asymmetric Gaussian is derived by the following steps. By definition:

$$\text{centroid in } x \text{ coordinate} = \frac{\int_a^b x f(x) dx}{\int_a^b f(x) dx}$$

When  $f(x)$  is a Gaussian with the center (the peak) at  $x = 0$ , the formula becomes

$$\text{centroid in } x \text{ coordinate} = \frac{\int_{-\infty}^{\infty} x \cdot e^{-1/2 (x/\sigma)^2} dx}{\int_{-\infty}^{\infty} e^{-1/2 (x/\sigma)^2} dx}$$

When a Gaussian has an asymmetric Gaussian profile with standard deviations  $\sigma_1$  and  $\sigma_2$  either side of the peak, the centroid is given by

centroid in  $x$  coordinate

$$= \frac{\int_{-\infty}^0 x \cdot e^{-1/2 (x/\sigma_1)^2} dx + \int_0^{\infty} x \cdot e^{-1/2 (x/\sigma_2)^2} dx}{\int_{-\infty}^0 e^{-1/2 (x/\sigma_1)^2} dx + \int_0^{\infty} e^{-1/2 (x/\sigma_2)^2} dx}$$

This is reduced to

centroid in  $x$  coordinate

$$= \frac{-\sigma_1^2 (1 - e^{-1/2 (\infty/\sigma_1)^2}) - \sigma_2^2 (e^{-1/2 (\infty/\sigma_2)^2} - 1)}{\sigma_1 \sqrt{\frac{\pi}{2}} + \sigma_2 \sqrt{\frac{\pi}{2}}}$$

and

$$e^{-1/2 (\infty/\sigma_1)^2} = 0$$

Therefore,

$$\begin{aligned} \text{centroid in } x \text{ coordinate} &= \frac{-\sigma_1^2 + \sigma_2^2}{\sigma_1 \sqrt{\frac{\pi}{2}} + \sigma_2 \sqrt{\frac{\pi}{2}}} \\ &= \sqrt{\frac{2}{\pi}} (\sigma_2 - \sigma_1) \end{aligned}$$

### Appendix B

Bandwidth of the stimuli

$\sigma$ Ratio	One-cycle Gabor	Two-cycle Gabor
0.6	0.68	0.34
1.0	0.50	0.25
1.4	0.42	0.21

The bandwidth of the asymmetric Gabor varied slightly with the  $\sigma$  ratio. The bandwidth (full-width at half height) is shown in octaves. As seen in the results depicted in Fig. 3, there is no clear relationship between the perceived shift and the bandwidth of an asymmetric Gabor.

### References

Badcock, D. R., Hess, R. F., & Dobbins, K. (1996). Localization of element clusters: multiple cues. *Vision Research*, 36, 1467–1472.

Finney, D. J. (1971). *Probit analysis*. Cambridge: Cambridge University Press.

Foster, D. H., & Bischof, W. F. (1991). Thresholds from psychometric functions: superiority of bootstrap to incremental and probit variance estimates. *Psychology Bulletin*, 109, 152–159.

Harris, J. P., & Fahle, M. (1995). The detection and discrimination of spatial offsets. *Vision Research*, 35, 51–58.

Hess, R. F., & Badcock, D. R. (1995). Metric for separation discrimination by the human visual system. *Journal of the Optical Society of America A*, 12, 3–16.

Hess, R. F., Dakin, S. R. G., & Badcock, D. R. (1994). Localization of element clusters by the human visual system. *Vision Research*, 34, 2439–2451.

Hess, R. F., & Hayes, A. (1994). The coding of spatial position by the human visual system: effects of spatial scale and eccentricity. *Vision Research*, 34, 625–643.

Hess, R. F., & Holliday, I. E. (1992). The coding of spatial position by the human visual system: spatial scale and contrast. *Vision Research*, 32, 1085–1097.

Hess, R. F., & Holliday, I. E. (1996). Primitives used in the spatial localization of nonabutting stimuli: peaks or centroids. *Vision Research*, 36, 3821–3826.

Klein, S. A., & Levi, D. M. (1985). Hyperacuity thresholds of 1 s: theoretical predictions and empirical validation. *Journal of the Optical Society of America A*, 2, 1170–1190.

Klein, S. A., & Levi, D. M. (1987). Position sense of the peripheral retina. *Journal of the Optical Society of America A*, 4, 1543–1553.

Kooi, F. L., DeValois, R. L., & Switkes, E. (1991). Spatial localization across channels. *Vision Research*, 31, 1627–1632.

Levi, D. M., & Klein, S. A. (1990). Equivalent intrinsic blur in amblyopia. *Vision Research*, 25, 979–991.

Levi, D. M., & Klein, S. A. (1992). Webers law for position: the role of spatial frequency and contrast. *Vision Research*, 32, 2235–2250.

Levi, D. M., & Tripathy, S. P. (1996). Localization of a peripheral patch: the role of blur and spatial frequency. *Vision Research*, 36, 3785–3803.

Levi, D. M., & Waugh, S. J. (1996). Position acuity with opposite-contrast polarity features: evidence for a nonlinear collector mechanism for position acuity? *Vision Research*, 36, 573–588.

Pelli, D. G., & Zhang, L. (1991). Accurate control of contrast on microcomputer displays. *Vision Research*, 31, 1337–1350.

Toet, A., & Koenderink, J. J. (1988). Differential spatial displacement discrimination thresholds for Gabor patches. *Vision Research*, 28, 133–143.

Waugh, S. J., & Levi, D. M. (1993). Visibility and Vernier acuity for separated targets. *Vision Research*, 33, 539–552.

Whitaker, D. (1993). What part of a Vernier stimulus determines performance? *Vision Research*, 33, 27–32.

Whitaker, D., McGraw, P. V., Pacey, I., & Barrett, B. T. (1997). Centroid analysis predicts visual localization of first- and second-order stimuli. *Vision Research*, 18, 2957–2970.

Whitaker, D., & MacVeigh, D. (1991). Interactions of spatial frequency and separation in Vernier acuity. *Vision Research*, 31, 1205–1212.

Wilson, H. R. (1986). Responses of spatial mechanisms can explain hyperacuity. *Vision Research*, 26, 453–469.

Wilson, H. R. (1991). Pattern discrimination, visual filters and spatial uncertainty. In M. Landy, & J. A. Movshon, *Computational models of visual processing*. Cambridge: MIT Press.